CHAPTER 6

Simulating Non-Linear Flows by using Newton-Raphson Technique

6.1 INTRODUCTION

The inclusion of non-Darcian flow and stress-dependent parameters leads to the non-linearity of the governing differential equation. In the previous chapters, while converting these nonlinear equations to algebraic equations (by finite difference scheme), the coefficient (additional) terms associated with the first and second-order spatial derivatives of *u* were evaluated at the previous (known) time step. Thereby, the nonlinear equations were forcibly converted into linear equations. Such as incorporating Elnaggar et al. (1973)'s exponential flow law, Terzaghi's one-dimensional consolidation equation gets converted into the following non-linear PDE:

$$\frac{k_u}{\gamma_w m_v}\frac{\partial^2 u}{\partial z^2}\underbrace{\left(1-(1-a)\theta\left[1-\exp\left(\frac{-\theta}{i_1\gamma_w}\frac{\partial u}{\partial z}\right)\right]\right)}_{E}+\frac{\partial q(t)}{\partial t}=\frac{\partial u}{\partial t} \tag{6.1}$$

Similar to the work of Liu et. al. (2009) and Li et. al. (2010), in the previous chapters, the hydraulic gradient within the exponential term was evaluated in the known time step. Thus, the section within the parenthesis (*E*) was turned into a constant number, resulting in the forced conversion of the nonlinear PDE into the linearized form. Thus, the task of obtaining the unknown solutions becomes straightforward through the formation of a simultaneous set of linear equations. Given the current computational flexibility, it does not seem to be prudent enough to simplify the *E*-term of the exponential component based on the previous time step.

An attempt has been made in this chapter to assess the advancement of the diffusion process by considering the *E*-term in the current (unknown) time step and thus avoiding forced linearization. The nonlinear equations generated through the finite difference discretization are solved by the employment of the Newton-Raphson technique. The present chapter focuses on the solutions process of the nonlinear method and aims to have an insightful observation of how and to what extent the consolidation process deviates due to the choice of two different time states (previous and current). The entire exercise aims to critically analyze the validity of the proposition that while incorporating the nonlinearity of *v-i* relationship, the time step at which the non-Darcian term is evaluated notably influences the prediction of the progress in the consolidation process.

A thorough investigation in this regard is carried out by employing the Barakat-Clark method (Barakat and Clark, 1966) and Crank-Nicolson implicit (Crank and Nicolson, 1947) schemes of Finite Difference Method (FDM) which converts the PDE into non-linear algebraic equations. The analyses are performed on a consolidating layer subjected to ramp loading and bounded by two different drainage conditions, namely, PTPB and PTIB. The deviation of the conventional and the present approaches are studied in terms of (i) normalized isochrones (curves between u/u_{max} and z/D_p) and (ii) consolidating curves (U_{avg} vs. T_v) as defined in Chapter 3.

6.2 FORMULATIONS AND ANALYSIS

Tables 6.1 and 6.2 present the algebraic formulations for computing the magnitude of u at each grid point, as shown in Fig. 4.1a (Chapter 4). The summary of the computational algorithm and their pictorial representation are depicted in Table 6.3 and Fig. 6.1, respectively. All the codes are written in *MATLAB* (version R2018A).

6.2.1 Crank Nicolson Implicit (CNI) Scheme

Following CNI scheme (refer Table 6.1), for any arbitrary i^{th} node, the basic governing equation (Eq. 6.1) gets converted into the algebraic equation, as mentioned in Eq. (6.2). Based on the considered t_m, Eq. (6.3) can be solved by using either of the following two approaches.

6.2.1.1 Conventional Approach -- Method A1: Considering $t_m = t$ (i.e. previous time step)

It is worth noting that if $t_m = t$, E_i^t includes all the known terms, and thus the algebraic equation (Eq. 6.1) for i^{th} node turns into the linearized form (Eq. 6.4). This eventually results in simultaneous set of linear equations, as given in Eq. (6.5). For Darcian flow, $E_i^t = 1$ and, therefore, the coefficient matrix (G) remains to be constant irrespective of time step. Conversely, for non-Darcian flow, G and H both the matrices vary with time.

6.2.1.2 Modified Approach -- Method A2: Considering $t_m = t + \Delta t$ (i.e. current time step)

Unlike the previous approach, $E_i^{t+\Delta t}$ remains to be unknown and therefore, the equations cannot be resolved into matrix form. Newton-Raphson iteration technique (Eq. 6.6) is employed for solving the nonlinear algebraic equations and updating the U vector at each time step. The forward time-marching scheme is illustrated in Fig. 6.1. In Method A1, the U-vector is updated all at once (i.e. in one operation) straightforwardly by the information of the previous time step, whereas, in Method A2, at any time step, U-vector is first initialized and then updated through the iterative scheme by using the Jacobian Matrix till the following stopping criterion is not achieved.

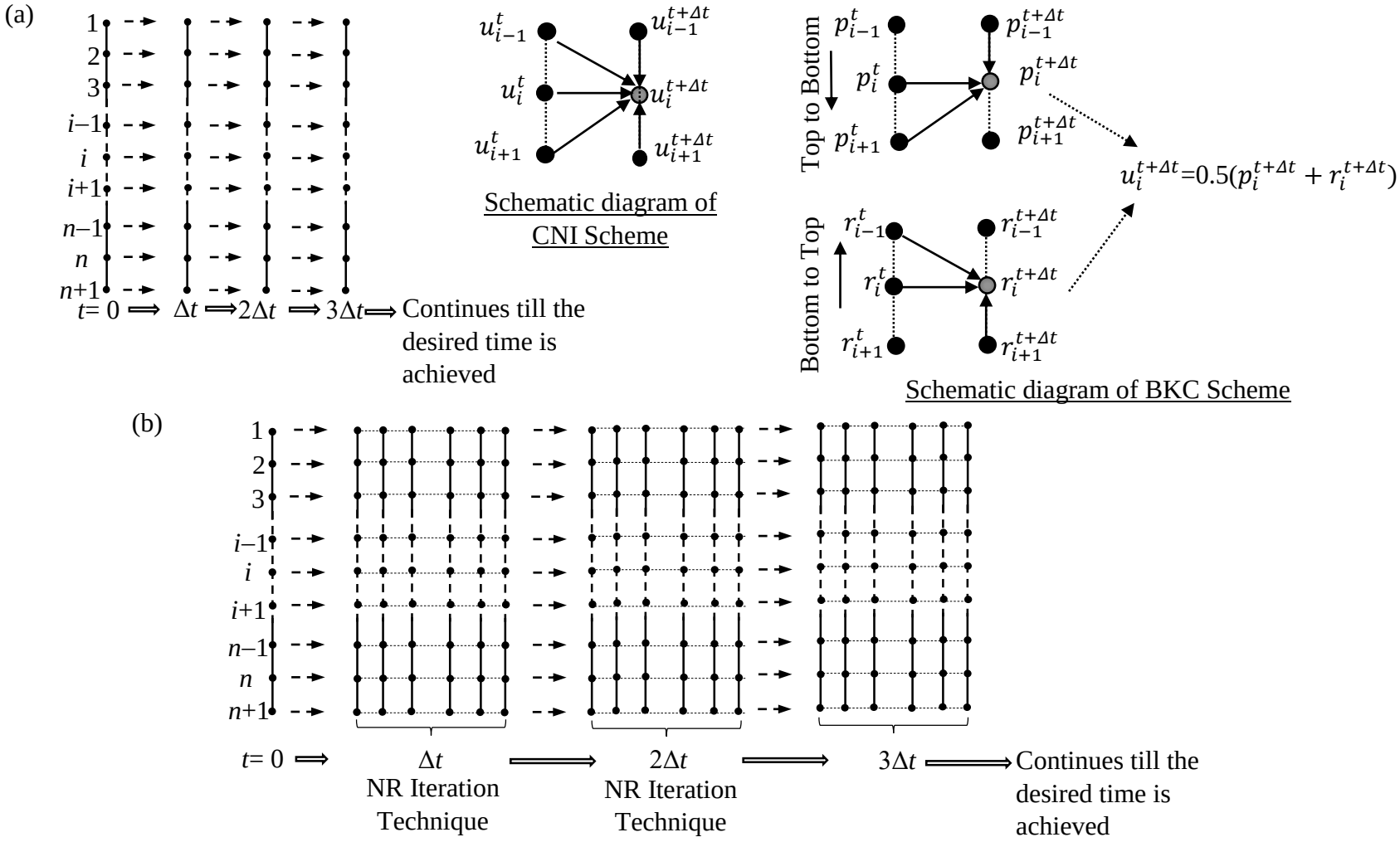

Fig. 6.1. Pictorial representation of the time marching scheme using the (a) conventional approach (Method A1/B1) and (b) modified approach (Method A2/B2).

6.2.2 Barakat–Clark (BKC) Method

In contrast to the conventional explicit method, BKC method (refer Table 6.2), the simplest Alternating Direction Explicit (ADE) scheme, is unconditionally stable (i.e. no restriction in λ) and is more reliable because the truncation errors involved in temporal and spatial directions are of second-order. Barakat and Clark (1966) in their classical paper advocated the use of this method from the standpoint of saving machine time, cost, and also increasing the accuracy of the solution. This method calculates the excess PWP at each time step (say, $t+\Delta t$), by simultaneously computing p_i's and r_i's from two opposite spatial directions, (as shown in Fig. 6.1); p_i's are calculated while moving along top to bottom direction, whereas, q_i's are calculated while moving along bottom to top direction. The magnitude of u_i is the average of p_i and q_i put together.

6.2.2.1 Conventional Approach -- Method B1: Considering $t_m = t$ (i.e. previous time step)

Similar to the conventional explicit method, here each equation involves only one unknown. As both the drainage boundary conditions are known, therefore, in any particular time step, p_i and r_i can be obtained explicitly from the above equations. However, it is to be noted that in contrast to the direct explicit method, the values of p_i's and r_i's need to be evaluated systematically.

6.2.2.2 Modified Approach-- Method B2: Considering $t_m = t + \Delta t$ (i.e. current time step)

Unlike Method B1, Eqs. (6.10) and (6.11) cannot be solved straightforwardly because each equation contains three unknowns. The equations are written for every node and the simultaneous non-linear equations are solved with the aid of Newton-Raphson technique as mentioned in Table 6.3.

Table 6.1 The form of the converted algebraic equation corresponding to different method of CNI scheme.

<table>
<tr><td rowspan="3">Crank Nicolson implicit (CNI)</td><td colspan="2">$$\frac{E_i^{tm}c_v}{2}\left(\frac{u_{i+1}^{t}-2u_i^{t}+u_{i-1}^{t}}{\Delta z^2}+\frac{u_{i+1}^{t+\Delta t}-2u_i^{t+\Delta t}+u_{i-1}^{t+\Delta t}}{\Delta z^2}\right)+\frac{q^{t+\Delta t}-q^{t}}{\Delta t}=\frac{u^{t+\Delta t}-u^{t}}{\Delta t} \quad (6.2)$$
here, (i) $E_i^{tm}=1-b_1\exp\left\{b_2\left(\frac{u_{i+1}-u_{i-1}}{2\Delta z}\right)\Big|_{@tm}\right\}$; $b_1=(1-a)\theta$, and $b_2=-\theta/i_1\gamma_w$, (ii) $c_v=\frac{k_u}{\gamma_w m_v}$
(iii) q^t = total applied pressure @ time t (iv) u_i^t = excess PWP @ time t corresponding to node i
(v) Δz = depth increment; Δt = time increment</td></tr>
<tr><td>Method A1</td><td>$$E_i^t\lambda\left(u_{i+1}^{t+\Delta t}-2u_{i+1}^{t+\Delta t}+u_{i+1}^{t+\Delta t}\right)+2\left(u_{i+1}^{t+\Delta t}-u_{i+1}^{t+\Delta t}\right)=2\left(u_{i+1}^{t+\Delta t}-u_{i+1}^{t+\Delta t}\right)-E_i^t\lambda\left(u_{i+1}^{t}-2u_{i+1}^{t}+u_{i-1}^{t}\right) \quad (6.3)$$ where, $\lambda=\frac{c_v\Delta t}{(\Delta z)^2}$
$$E_i^t=1-b_1\exp\left\{b_2\left(\frac{u_{i+1}^t-u_{i-1}^t}{2\Delta z}\right)\right\}$$
$$\Rightarrow -E_i^t\lambda u_{i+1}^{t+\Delta t}+2\left(1+E_i^t\lambda\right)u_i^{t+\Delta t}-E_i^t\lambda u_{i-1}^{t+\Delta t}=-E_i^t\lambda u_{i+1}^{t}+2\left(1+E_i^t\lambda\right)u_i^{t}-E_i^t\lambda u_{i-1}^{t}-2\left(q^{t+\Delta t}-q^{t}\right) \quad (6.4)$$
Eq. 6.4 can be further resolved into the following: $GU=H$; G, U and H are written in Appendix D1 (6.5)</td></tr>
<tr><td>Method A2</td><td>$\boldsymbol{g}$: $$\lambda E_i^{t+\Delta t}\left(u_{i+1}^{t}-2u_i^{t}+u_{i-1}^{t}+u_{i+1}^{t+\Delta t}-2u_i^{t+\Delta t}+u_{i-1}^{t+\Delta t}\right)+2\left(q^{t+\Delta t}-q^{t}-u_i^{t+\Delta t}+u_i^{t}\right) \quad (6.6)$$
Note: Here the function, $\boldsymbol{g_i}$ depends on: (i) known and unknown field variables, (ii) λ, (iii) model parameters (a, θ, and i_1), and (iv) loading parameters ($q^{t+\Delta t}, q^t$).</td></tr>
</table>

Table 6.2 The form of the converted algebraic equation corresponding to different method of BKC scheme.

<table>
<tr><td rowspan="4">Alternating Direction Explicit (ADE) --BKC</td><td colspan="2">When, i runs from 2 to n (top to bottom): $\frac{c_v}{2}\left(\frac{p_{i-1}^{t+\Delta t}-p_i^{t+\Delta t}-p_i^t+p_{i+1}^t}{(\Delta z)^2}\right)\left[1-b_1\exp\left\{b_2\left(\frac{p_{i+1}-p_{i-1}}{2\Delta z}\right)\Big|_{@tm}\right\}\right]+\frac{q^{t+\Delta t}-q^t}{\Delta t}=\frac{p_i^{t+\Delta t}-p_i^t}{\Delta t}$ (6.7a)</td></tr>
<tr><td colspan="2">When, i runs from n to 2 (bottom to top): $\frac{c_v}{2}\left(\frac{r_{i-1}^t-r_i^t-r_i^{t+\Delta t}+r_{i+1}^{t+\Delta t}}{(\Delta z)^2}\right)\left[1-b_1\exp\left\{b_2\left(\frac{r_{i+1}-r_{i-1}}{2\Delta z}\right)\Big|_{@tm}\right\}\right]+\frac{q^{t+\Delta t}-q^t}{\Delta t}=\frac{r_i^{t+\Delta t}-r_i^t}{\Delta t}$ (6.7b)</td></tr>
<tr><td colspan="2">The value of $u_i^{t+\Delta t}$ is then evaluated by averaging technique: $u_i^{t+\Delta t}=\frac{1}{2}\left(p_i^{t+\Delta t}+r_i^{t+\Delta t}\right)$ (6.8)
Appendix D illustrates the detail calculation process.</td></tr>
<tr><td>Method B1</td><td>$p_i^{t+\Delta t}=C_1\left(p_{i-1}^{t+\Delta t}+p_{i+1}^t\right)+D_1p_i^t+E_1(q^{t+\Delta t}-q^t)$; $r_i^{t+\Delta t}=C_2(r_{i+1}^{t+\Delta t}+r_{i-1}^t)+D_2r_i^t+E_2(q^{t+\Delta t}-q^t)$ (6.9)
where, $C_1=\frac{\lambda N_i^t}{(2+\lambda N_i^t)}$; $D_1=\frac{(2-\lambda N_i^t)}{(2+\lambda N_i^t)}$; $E_1=\frac{2}{(2+\lambda N_i^t)}$: $N_i^t=1-b_1\exp\left\{b_2\left(\frac{p_{i+1}^t-p_{i-1}^t}{2\Delta z}\right)\right\}$
$C_2=\frac{\lambda S_i^t}{(2+\lambda S_i^t)}$; $D_2=\frac{(2-\lambda S_i^t)}{(2+\lambda S_i^t)}$; $E_2=\frac{2}{(2+\lambda S_i^t)}$: $S_i^t=1-b_1\exp\left\{b_2\left(\frac{r_{i+1}^t-r_{i-1}^t}{2\Delta z}\right)\right\}$</td></tr>
<tr><td>Method B2</td><td>$\boldsymbol{h_{1i}}:\lambda\left(p_{i-1}^{t+\Delta t}-p_i^{t+\Delta t}-p_i^t+p_{i+1}^t\right)\left[1-b_1\exp\left\{b_2\left(\frac{p_{i+1}^{t+\Delta t}-p_{i-1}^{t+\Delta t}}{2\Delta z}\right)\right\}\right]+2\left(q^{t+\Delta t}-q^t-p_i^{t+\Delta t}-p_i^t\right)=0$ (6.10)
$\boldsymbol{h_{2i}}:\lambda\left(r_{i-1}^t-r_i^t-r_i^{t+\Delta t}+r_{i+1}^{t+\Delta t}\right)\left[1-b_1\exp\left\{b_2\left(\frac{r_{i+1}^{t+\Delta t}-r_{i-1}^{t+\Delta t}}{2\Delta z}\right)\right\}\right]+2\left(q^{t+\Delta t}-q^t-r_i^{t+\Delta t}-r_i^t\right)=0$ (6.11)
Here the function, $\boldsymbol{h_{1i}}$, and $\boldsymbol{h_{2i}}$ depends on: (i) known and unknown field variables, (ii) λ, (iii) model parameters (a, θ, and i_1), and (iv) loading parameters ($q^{t+\Delta t}, q^t$).</td></tr>
</table>

Table 6.3 Stepwise algorithm of CNI and ADE scheme.

	CNI	ADE
Considering $t_m = t$	*Step 1*: $GU^{t+\Delta t} = H$; here, G and H are function of known vector, U^t. *Step 2*: $GU^{t+2\Delta t} = H$; here, G and H are functions of vector $U^{t+\Delta t}$, obtained from Step-1. *Step 3*: $GU^{t+3\Delta t} = H$; here, G and H are functions of vector $U^{t+2\Delta t}$, obtained from Step-2. and the process continues till the desired time step is reached.	*Step 1*: Using Eq. 6.6, obtain $\boldsymbol{P}$ and $\boldsymbol{R}$ and compute $\boldsymbol{U}$ @ time step $t+\Delta t$. $\boldsymbol{P}^{t+\Delta t} = \left\{ p_2^{t+\Delta t} \quad p_3^{t+\Delta t} \quad p_4^{t+\Delta t} \quad \ldots \quad \ldots \quad p_{n-2}^{t+\Delta t} \quad p_{n-1}^{t+\Delta t} \quad p_n^{t+\Delta t} \right\}^T$ $\boldsymbol{R}^{t+\Delta t} = \left\{ r_2^{t+\Delta t} \quad r_3^{t+\Delta t} \quad r_4^{t+\Delta t} \quad \ldots \quad \ldots \quad r_{n-2}^{t+\Delta t} \quad r_{n-1}^{t+\Delta t} \quad r_n^{t+\Delta t} \right\}^T$ $U = 1/2(\boldsymbol{P}+\boldsymbol{R})$; *Step 2*: Similarly, obtain $\boldsymbol{P}$ and $\boldsymbol{R}$ and compute $\boldsymbol{U}$ @ time step $t+2\Delta t$. And the process will continue till the desired time step is reached.
Considering $t_m = t + \Delta t$	*Step 1*: Assume U @ time step $t+\Delta t$. *Step 2*: Compute modified U through the following equation: $U_{new} = U_{previous} - J^{-1} G_k$; *Step 3*: Check whether $diff\left(= \sqrt{\sum_{i=1}^{n+1} \left(u_i^{t+\Delta t}\big\vert_{new} - u_i^{t+\Delta t}\big\vert_{previous} \right)^2} \right) < tolerance$ or not. *Step 4*: If the convergence criterion in Step 3 is not satisfied, assign $U_{previous} = U_{new}$ and repeat Step2. Else, continue to Step 5. Step-5: Proceed to the next time step $t+2\Delta t$. Note: The form of the Jacobian matrix, $\boldsymbol{J}$ and the vector $\boldsymbol{G}$, is mentioned in Appendix D2.	*Step 1*: Assume $\boldsymbol{P}$ and $\boldsymbol{Q}$ @ time step $t+\Delta t$. *Step 2*: Compute modified $\boldsymbol{P}$ and $\boldsymbol{Q}$ through the following equation: $\boldsymbol{P}_{new} = \boldsymbol{P}_{previous} - \boldsymbol{J}_1^{-1} \boldsymbol{G}_1$; $\boldsymbol{R}_{new} = \boldsymbol{R}_{previous} - \boldsymbol{J}_2^{-1} \boldsymbol{G}_2$; *Step 3*: Check whether $diff\left(= \sqrt{\sum_{i=1}^{n+1} \left(p_i^{t+\Delta t}\big\vert_{new} - p_i^{t+\Delta t}\big\vert_{previous} \right)^2} \right) < tolerance$ or not. $diff\left(= \sqrt{\sum_{i=1}^{n+1} \left(r_i^{t+\Delta t}\big\vert_{new} - r_i^{t+\Delta t}\big\vert_{previous} \right)^2} \right) < tolerance$ or not. *Step 4*: If the inequality constraint in Step 3 is not satisfied, assign $\boldsymbol{P}_{previous} = \boldsymbol{P}_{new}$, $\boldsymbol{R}_{previous} = \boldsymbol{R}_{new}$ and repeat Step2. Else, continue to Step 5. *Step 5*: Obtain vector U by averaging out the $\boldsymbol{P}_{new}$ and $\boldsymbol{R}_{new}$ *Step 6*: Proceed to the next time step $t+2\Delta t$. Note: The form of the Jacobian matrices (J_1 and J_2), and the vectors, G_1, and G_2 are mentioned in Appendix D3

Note: In the present manuscript, *tolerance* is chosen as 10^{-4} for all the cases.

6.3 NUMERICAL VERIFICATION

6.3.1 Problem Statement

An isotropic, homogenous, saturated clay layer of thickness, *H*, is subjected to a time-dependent ramp loading (as shown in Chapter 4). The excess PWP, generated due to the application of external load, dissipates over time following every assumption of Terzaghi`s 1D consolidation theory (e.g. stress independent permeability and compressibility characteristics, small strains, uniform distribution of initial excess PWP and the total stress along the depth) except the Darcian law. Unlike the problem statement in Chapter 4, the material parameters are stress-independent. The non-linear relation between flow velocity and hydraulic gradient is modeled through Eq. 6.1. It is intended to understand that how these four different approaches (Methods A1, A2, B1, and B2), influence the consolidation behaviour of the chosen clayey stratum. The model parameters and loading rate are extensively varied.

6.4 RESULTS AND INTERPRETATIONS

Upon solving an unsteady, one- and two-dimensional heat diffusion problem, it was reported Barakat and Clark (1966) that in comparison with the Crank–Nicolson method, the results obtained from the BKC method are in better agreement with the exact solutions. It was also observed that for obtaining modest accuracy in the approximating solutions, CNI scheme requires quite a large number of iterations per time step which may result in high computational time in comparison with any of the explicit technique. Although this article primarily focuses on establishing the influence of chosen time state at which the additional term of nonlinear flow is computed, however, for the sake of completeness, a comparison between both the schemes is drawn on a consolidating layer subjected to constant loading and they are presented in Fig. 6.2 and Table 6.4.

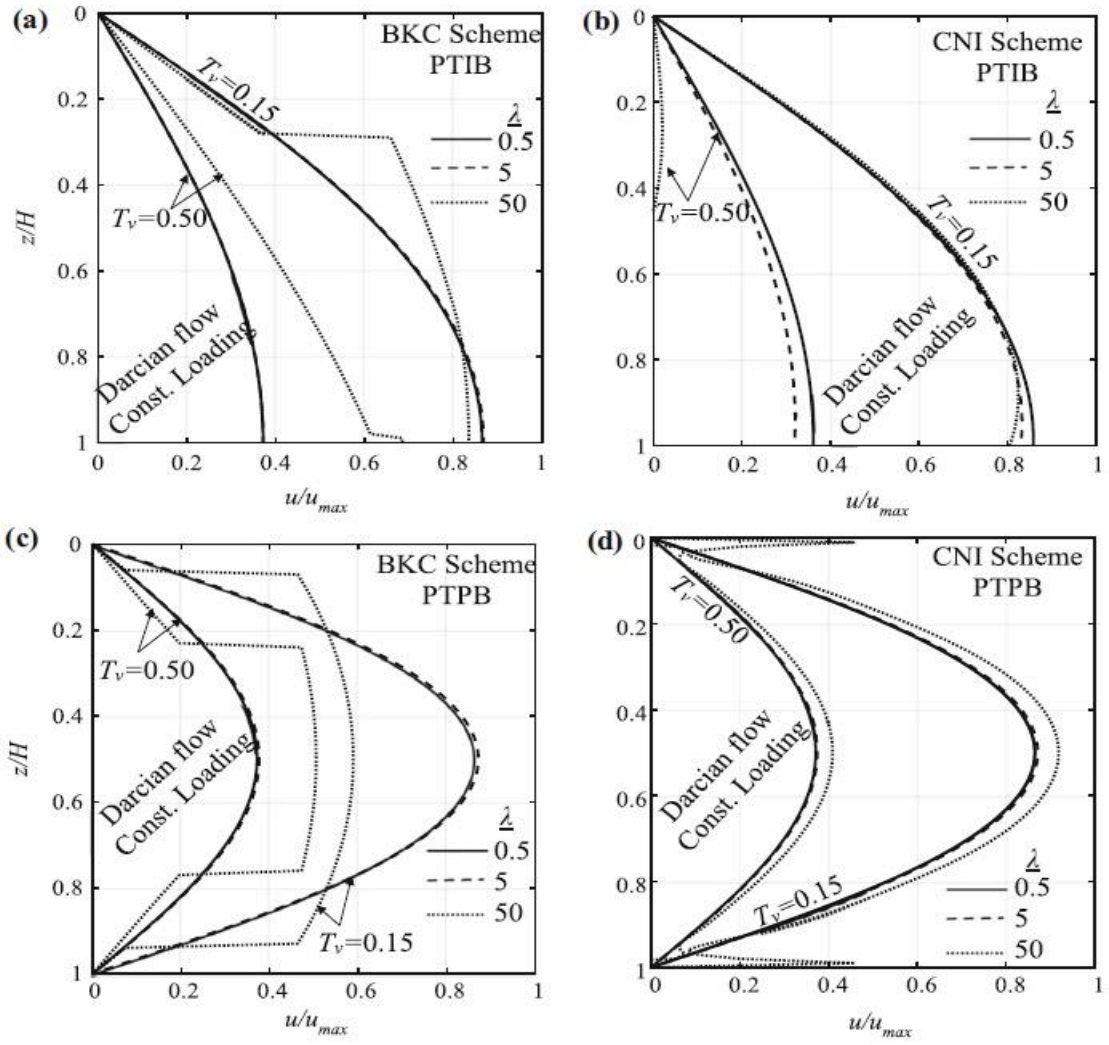

Fig 6.2 Comparisons of the normalized isochrones for different λ and obtained from different finite difference schemes, namely, (a), (c) BKC and (b), (d) CNI

Corresponding to various λ, the excess PWP values retained at mid-point (PTPB) and bottommost point (PTIB) are reported in Table 6.4. It is observed that even for λ = 20, CNI scheme provides consistent solution but BKC method fails to do so. Fig. 6.2 shows that if λ is considered to be 50, the isochrones emerge from CNI scheme is still not so bad, especially for the PTPB condition. However, the isochrones from BKC for λ = 50 are not at all in accordance with the expected solutions. This indicates that the restriction on the value of λ can be relaxed to a great extent in case of CNI scheme.

Table 6.4 The comparison of *u* from CNI and BKC schemes

λ	Excess pore water pressure, *u*			
	PTPB (Measured @ mid-point and @T_v=0.4		PTIB (Measured @ bottom most-point and @ T_v =0.1	
	CNI Scheme	BKC Scheme	CNI Scheme	BKC Scheme
1	47.50	47.51	94.48	94.95
5	47.78	48.15	93.00	95.02
10	48.13	49.74	90.65	94.76
20	48.85	64.18	90.25	92.37

To present the deviation of the proposed modified and the conventional formulations of non-Darcian flow law, the normalized PWP isochrones and the consolidation curves are obtained from CNI schemes by varying model parameters, loading rate and drainage boundary conditions.

It is to be noted that for the chosen λ (= 0.75), there is negligible difference between the solutions obtained by BKC and CNI method. Corresponding to two different construction time (T_{vc} = 0.01 and 0.1) and at two different time factors (T_v), namely, 0.4 and 0.6, Figs. 6.3 and 6.4 depict the normalized PWP isochrones subjected to PTPB and PTIB conditions, respectively.

In these figures, the terms DF, NDF1, and NDF2 indicate the curves generated from Darcian law, and non-Darcian flow using Method A1 and A2, respectively. It can be clearly observed from these figures that irrespective of the hydraulic drainage boundary conditions, the retained amount of excess PWP in the entire consolidating layer (i.e. the area encompasses by the isochrones) is always smaller for Darcian flow. This implies that the Darcian flow law over predicts the consolidation rate than its nonlinear counterpart. As the flow rule becomes linear (i.e. a= 1, and/or θ =0), the deviation between Darcian and non-Darcian curves vanishes. It is invariably observed from the figures that no matter

whatever be the drainage condition or the nonlinear flow parameters, the NDF1 (dashed) lines always lie between the DF (dotted) and the NDF2 (solid) lines. These results give a clear impression that the analyses performed by Method A1 show faster rate of consolidation than Method A2. The difference between NDF1 and NDF2 curves becomes quite significant as the nonlinearity of v vs. i relationship increases either by reducing a and/or by increasing θ. The curves also show that the changes in θ parameter mainly impact the NDF2 curves, whereas variation in a influences both the non-Darcian (NDF1 and NDF2) curves. With the advancement in consolidation process, this deviation further widens up for both type of hydraulic drainage boundaries. Furthermore, the impact of i_1 parameter can be read by comparing Figs. 6.3b, e, and 6.4b, e. It is well observed that NDF1 curves shift towards the DF lines with the suppression of the i_1 value.

Figs 6.5 and 6.6 clearly depict that for any specific model parameters, the deviation of the NDF1 and NDF2 settlement curves is maximum for the instantaneous loading and reduces with the slow loading rate. For any loading rate, NDF1 curves shift towards DF if either the value of a or i_1 is lower or the value of θ is higher. Past studies showed that the Darcian flow law predicts faster rate of PWP dissipation. This article further shows that in contrast to the conventional approach if non-Darcian flow law is analyzed by the proposed modified approach, then the process of primary consolidation appears to progress at a delayed rate.

6.5 VERIFICATION

Table 6.5 shows the comparison of the present numerical solutions with the solutions reported by Lovisa et al. (2010) for PTPB and PTIB drainage conditions subjected to Darcian flow. The close proximity (variation ranges between 0.01% - 3%.) between these solutions provide the necessary confidence on the methodology and the written code.

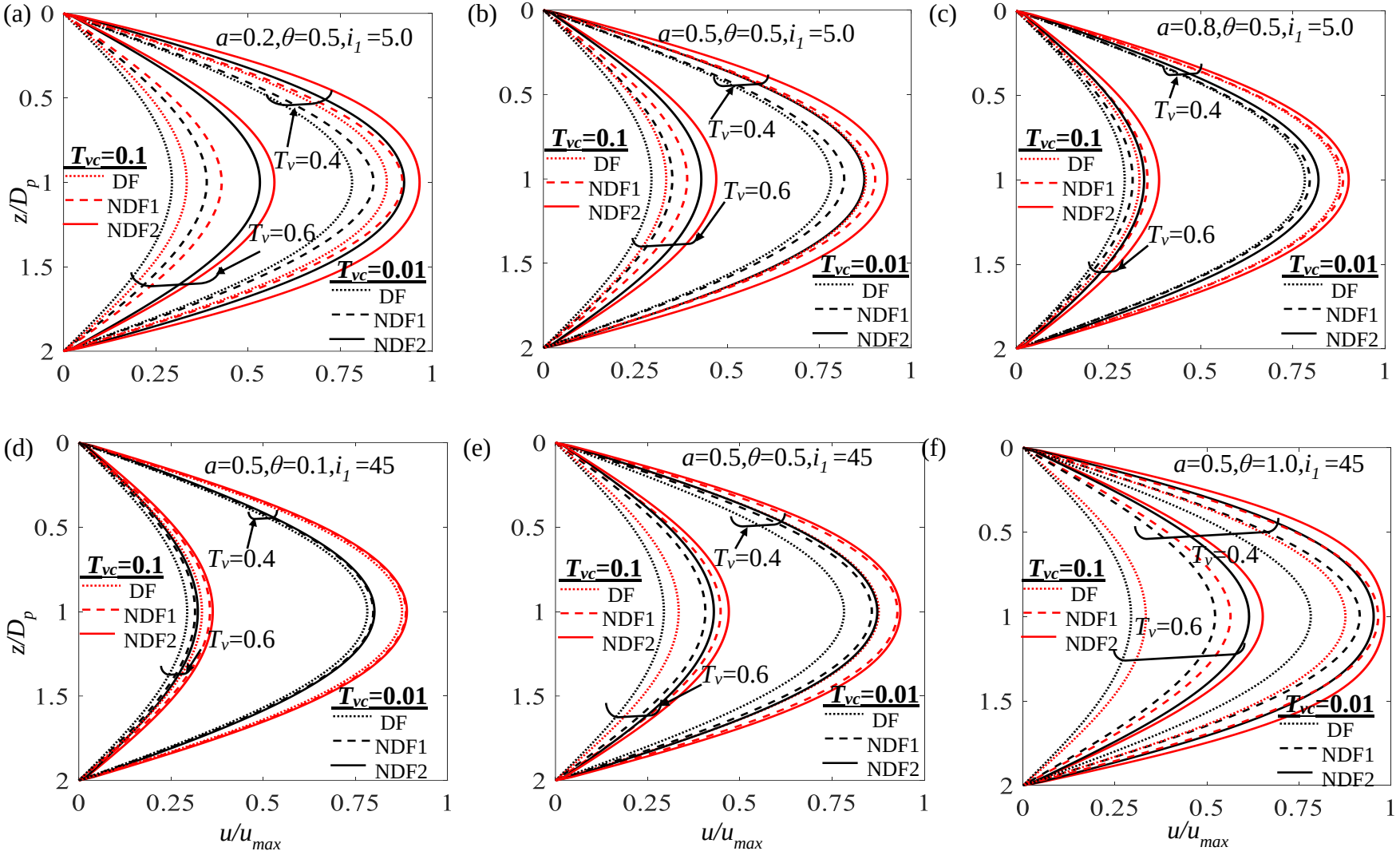

Fig. 6.3 Normalized isochrones for PTPB plotted at two different time and correspond to various model parameters and two different construction time factors (T_{vc}), namely, 0.01 and 0.1.

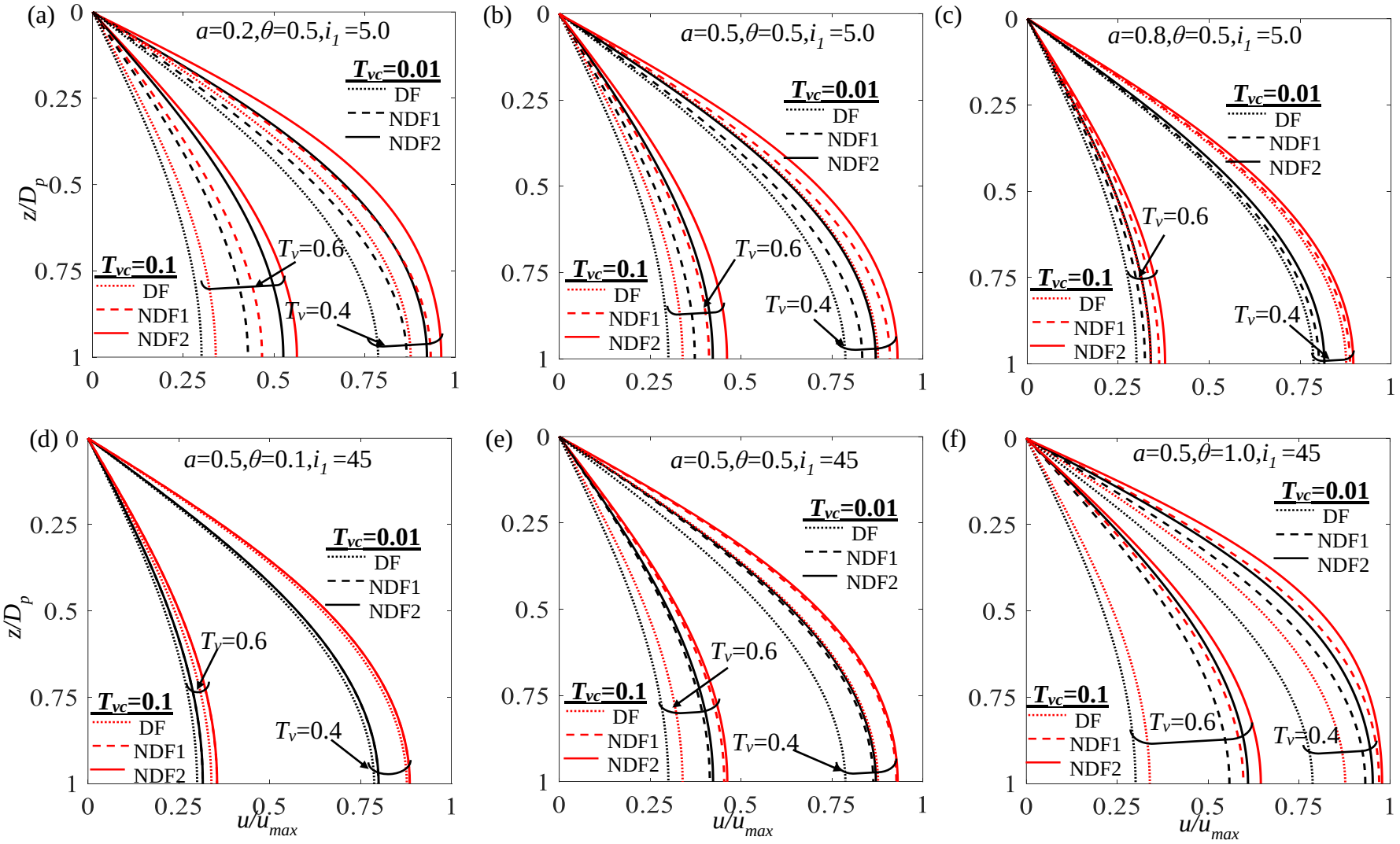

Fig. 6.4 Normalized isochrones for PTIB plotted at two different time and correspond to various model parameters and two different construction time factors (T_{vc}), namely, 0.01 and 0.1.

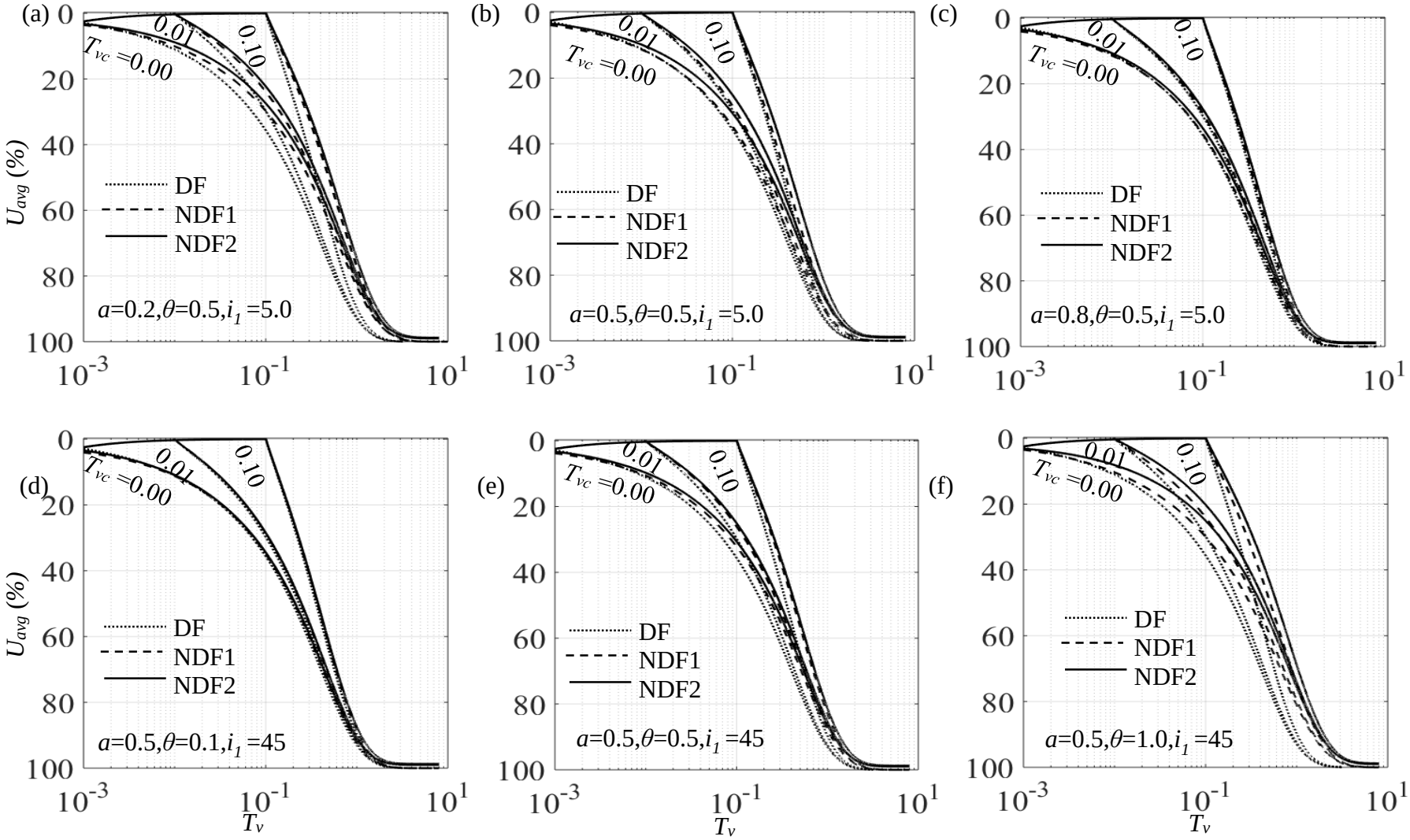

Fig. 6.5 Consolidating curves for PTPB correspond to various model parameters and three different construction time factors (T_{vc}), namely,0.00, 0.01, and 0.1.

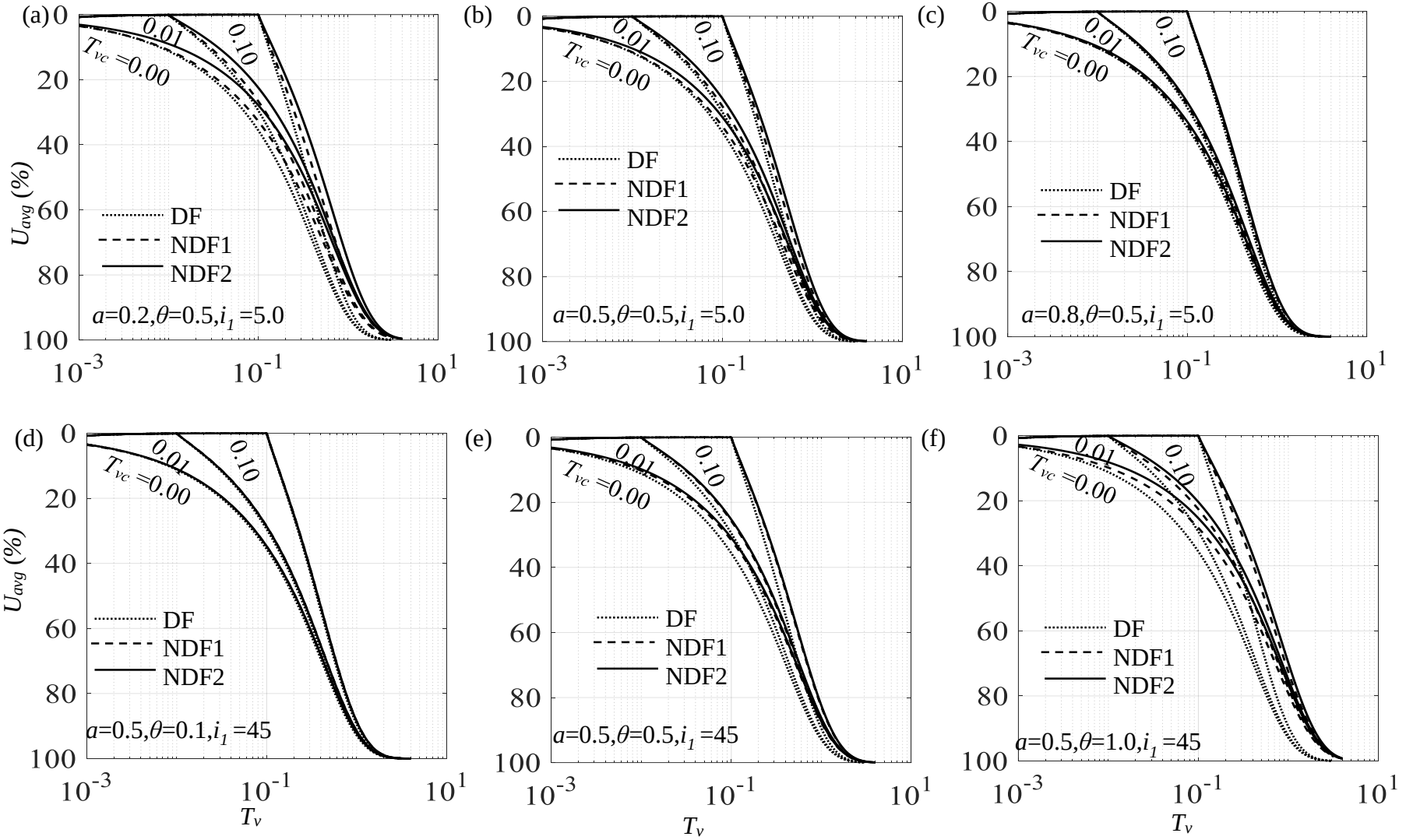

Fig. 6.6 Consolidating curves for PTIB correspond to various model parameters and three different construction time factors (T_{vc}), namely, 0.00, 0.01, and 0.1.

Table 6.5. A comparison of the present solutions with the solutions computed by Lovisa et al. (2010) and (2012)

T_v	Average degree of consolidation			
	PTPB		PTIB	
	Lovisa et al. (2010)	DF	Lovisa et al. (2012)	DF
0.001	0.0331	0.0345	0.0429	0.0409
0.010	0.1126	0.1132	0.1712	0.1628
0.100	0.3581	0.3536	0.4593	0.4568
0.200	0.4952	0.4987	0.5983	0.5941
0.400	0.6999	0.6909	0.7476	0.7279
0.600	0.8022	0.8074	0.8489	0.8255
0.800	0.8835	0.8785	0.9038	0.8874
1.000	0.9254	0.9220	0.9381	0.9313

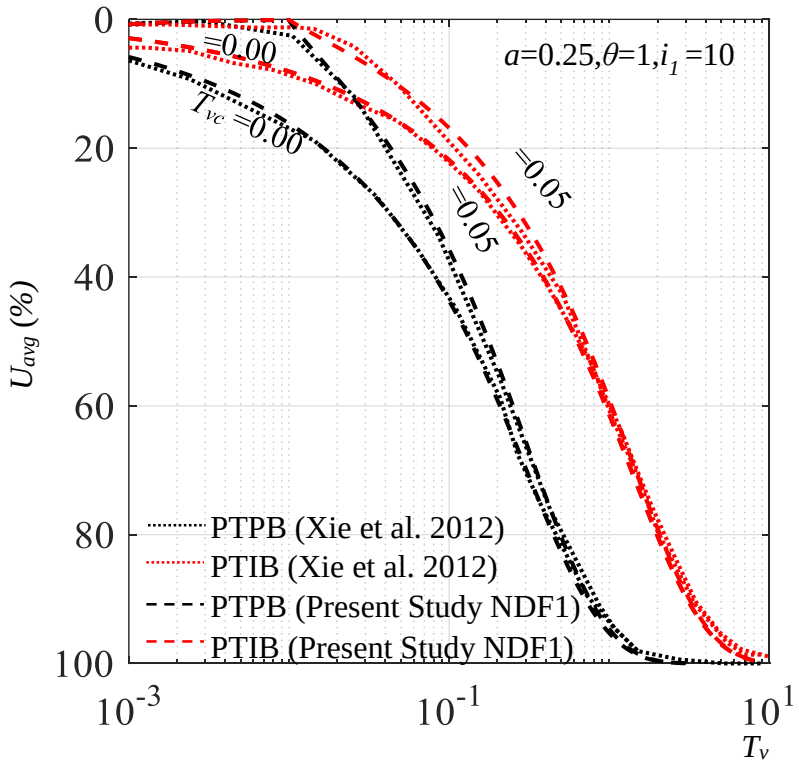

Fig.6.7 A comparison of the present numerical solutions with the numerical solutions presented by Xie et al. 2012.

The NDF1 curves obtained in the present articles are further compared with the numerical solutions provided by Xie et al. (2012) for a specific non-Darcian flow (a=0.25, θ=1 and i_1=10) and corresponding to two different values of T_{vc}, namely, 0 and 0.05. The comparison is presented in Fig. 6.7. The curves coincide with each other for the constant loading (T_{vc}=0); however, for ramp loading (T_{vc}=0.05) a small amount of deviation is visible in the initial stage of consolidation, especially for the single drainage condition. This may be because of the difference in the chosen increment factors, version of the computational tool etc.

6.6 SUMMARY

In this chapter, an attempt has been made to analyze the consolidation behaviour of one-dimensional clayey soil by considering the non-linear diffusion equation in its proper form, unlike the forced linearization as in traditional approach. Two different finite difference schemes – alternating explicit Barakat-Clarke method and semi-implicit Crank Nicolson method – are implemented for the numerical simulations. The fluid flow is modelled through the four-parameter-dependent non-Darcian model. During the forward time-marching, the pore water pressure vector is updated by following the gradient-based Newton-Raphson iterative technique. The deviation of the present and the conventional approaches are minutely examined.